

Critical behavior of the 3d random field Ising model: Two-exponent scaling or first order phase transition?

Heiko Rieger

Institut für Theoretische Physik, Universität zu Köln, 50926 Köln, Germany

and

HLRZ c/o Forschungszentrum Jülich, Postfach 1913, 52425 Jülich, Germany

(March 7, 1995)

In extensive Monte Carlo simulations the phase transition of the random field Ising model in three dimensions is investigated. The values of the critical exponents are determined via finite size scaling. For a Gaussian distribution of the random fields it is found that the correlation length ξ diverges with an exponent $\nu = 1.1 \pm 0.2$ at the critical temperature and that $\chi \sim \xi^{2-\eta}$ with $\eta = 0.50 \pm 0.05$ for the connected susceptibility and $\chi_{\text{dis}} \sim \xi^{4-\bar{\eta}}$ with $\bar{\eta} = 1.03 \pm 0.05$ for the disconnected susceptibility. Together with the amplitude ratio $A = \lim_{T \rightarrow T_c} \chi_{\text{dis}} / \chi^2 (h_r/T)^2$ being close to one this gives further support for a two exponent scaling scenario implying $\bar{\eta} = 2\eta$. The magnetization behaves discontinuously at the transition, i.e. $\beta = 0$, indicating a first order transition. However, no divergence for the specific heat and in particular no latent heat is found. Also the probability distribution of the magnetization does not show a multi-peak structure that is characteristic for the phase-coexistence at first order phase transition points.

75.10.H, 05.50, 64.60.C

I. INTRODUCTION

The critical behavior of the random field Ising model (RFIM) has been investigated intensively over two decades now (see¹ for a review) but a full agreement over the most fundamental issues still missing. Although it has been shown rigorously² that at low temperatures and sufficiently small field strength there is indeed long range ferromagnetic order in three dimensions, the characterization of the phase transition is still unclear. The idea of dimensional reduction³ failed to describe the critical behavior of the model correctly. The reason for this was essentially the presence of many local minima in the free energy landscape that do not allow for a straightforward perturbative treatment. A reminiscence of dimensional reduction is still present in the scaling theories for the RFIM⁴⁻⁶, where the dimension d has been replaced by $d - \theta$ in hyper-scaling relations and θ was introduced as a third exponent independent of ν and η . However, these (droplet)-theories relied upon the assumption of a second order phase transition. Part of the results obtained via Monte Carlo simulations support this scenario^{8,7}, whereas other simulations find indications for the transition to be of first order^{9,10}. More surprisingly no latent heat was found at the transition¹⁰, contrary to what one might expect at a first order phase transition¹¹, where a discontinuity in the internal energy at the critical point causes the specific heat to diverge with the volume of the system. Actually no divergence at all could be detected for the specific heat¹⁰.

The experimental situation is also far from clear. Experiments on diluted antiferromagnets in an uniform external field (DAFF), which have been demonstrated to be in the same universality class as the RFIM^{12,13}, pro-

vided evidence for a second order phase transition with varying estimates for the critical exponents (for a discussion see¹). In¹⁴ a logarithmic singularity for the specific heat was found, implying $\alpha = 0$. Quite recently, subsequent to the prediction made in¹⁰, experimental evidence of a cusp-like singularity of the specific heat, i.e. $\alpha < 0$, was reported¹⁵. Moreover, other possible scenarios, like a first order transition¹⁶ or a so called “trompe l’oeil critical behavior”¹⁷ have also been discussed. Experiments addressing the equilibrium quantities of the RFIM (or the DAFF, respectively) are extremely difficult to perform, since by approaching the transition the system falls out of equilibrium very rapidly and freezes into a metastable domain state (see¹⁸ for a review). Therefore these issues have not been settled by now.

The purpose of this paper is to estimate *all* critical exponents with the help of extensive Monte Carlo investigations of the RFIM in three dimensions. In a recent paper results for the exponents of the RFIM with a binary distribution were presented¹⁰. In mean field theory¹⁹ there is a sharp discrepancy between the phase diagram for a binary distribution and that of a continuous distribution with a finite probability for zero random fields: in the former case the phase diagram has a tricritical point, where the phase transition changes from second order for low fields to first order at higher fields; in the latter case the transition is always of second order. One might speculate that a similar scenario occurs also in three dimensions and that the indications found in¹⁰ for a first order transition are in fact an artifact of the binary distribution. Therefore it is important to perform a similar analysis for a continuous distribution, which is presented in this paper.

It is organized as follows: In section 2 we present the model and review various scaling predictions that are

supposed to hold in case the transition is of second order. Section 3 reports our results of the finite size scaling analysis and section 4 discusses the possibility of a first order transition. Section 5 is a summarize and an outlook.

II. MODEL AND SCALING THEORY

The random field Ising model (RFIM) in three dimensions is defined by the Hamiltonian

$$H = -J \sum_{\langle i,j \rangle} S_i S_j - \sum_i h_i S_i, \quad (1)$$

where $S_i = \pm 1$ are Ising spins, the first sum is over nearest neighbor pairs on a simple cubic lattice and the h_i are independent quenched random variables with mean zero $[h_i]_{\text{av}} = 0$ and variance $[h_i^2]_{\text{av}} = h_r^2$. It has been shown rigorously² that this model has a transition to long range ferromagnetic order along a line $h_r(T)$ in the (h_r, T) -diagram.

If this transition is second order, a scaling theory has been proposed⁴⁻⁶ that relies upon the assumption that random field induced fluctuations dominate over thermal fluctuations at T_c . This implies for the singular part of the free energy

$$F_{\text{sing}} \sim \xi^\theta, \quad (2)$$

where ξ is the correlation length diverging at the critical temperature like

$$\xi \sim t^{-\nu} \quad \text{with} \quad t = T - T_c \quad (3)$$

and θ is a new exponent. Random field fluctuations alone produce typically an excess field of the order of $\xi^{d/2}$ within a correlation volume, so a naive guess would be θ roughly 1.5 in three dimensions. From (2) the modified hyper-scaling relation follows

$$2 - \alpha = \nu(d - \theta), \quad (4)$$

α being the specific heat exponent. It also implies an exponential divergence of the relaxation time τ at T_c : $\tau \sim \exp(A\xi^\theta)$. The decay of the connected and disconnected correlation functions at T_c

$$C(\mathbf{r}) = [\langle S_0 S_r \rangle - \langle S_0 \rangle \langle S_r \rangle]_{\text{av}} \sim r^{-(d-2+\eta)} \quad (5)$$

$$C_{\text{dis}}(\mathbf{r}) = [\langle S_0 \rangle \langle S_r \rangle]_{\text{av}} \sim r^{-(d-4+\bar{\eta})} \quad (6)$$

defines two exponents η and $\bar{\eta}$. These are expected^{4,5} to be related to the new exponent θ via

$$\theta = 2 - \bar{\eta} + \eta. \quad (7)$$

By approaching the critical temperature from above the corresponding connected and disconnected susceptibilities diverge as

$$\chi = \int d\mathbf{r} C(\mathbf{r}) \sim (T - T_c)^{-\gamma}, \quad (8)$$

$$\chi_{\text{dis}} = \int d\mathbf{r} C_{\text{dis}}(\mathbf{r}) \sim (T - T_c)^{-\bar{\gamma}}. \quad (9)$$

These exponents are related by

$$\gamma = \nu(2 - \eta), \quad (10)$$

$$\bar{\gamma} = \nu(4 - \bar{\eta}). \quad (11)$$

In addition one has the usual scaling relations for the magnetization exponent

$$\beta = (d - 4 + \bar{\eta}), \quad (12)$$

and the Rusbrooke equality

$$\alpha + 2\beta + \gamma = 2. \quad (13)$$

Obviously there seem to be three independent critical exponents and a central issue of the activities on the critical properties of the RFIM is the quest for an additional scaling relation. Already Imry and Ma²⁰ conjectured that $F_{\text{sing}} \sim \chi$, where $\chi \sim (T - T_c)^{-\gamma}$ is the susceptibility. This would imply $\theta = 2 - \eta$ via (2) and therefore with (7)

$$\bar{\eta} = 2\eta. \quad (14)$$

A set of analytical arguments by Schwartz et al.^{21,22} supports this two-exponent scaling scenario indicated by (14). Hence the exact Schwartz-Soffer inequality²¹ $\bar{\eta} \leq 2\eta$ might be fulfilled as an equality, as in (14). A recent high temperature series analysis provided²³ strong evidence of this equality to hold by estimating γ and $\bar{\gamma}$ via Padé-approximation.

In this paper we intend to determine *all* critical exponents with Monte Carlo simulations. The model is defined by the Hamiltonian (1) on a finite lattice of linear size L with periodic boundary conditions. Instead of a binary distribution, as used in¹⁰, we consider here a Gaussian distribution

$$P(h_i) = \frac{1}{\sqrt{2\pi h_r^2}} \exp(-h_i^2/2h_r^2) \quad (15)$$

for the random fields. Unfortunately this makes the use of multispin coding impossible²⁴, which slows down the spin-update algorithm (Metropolis) by approximately a factor 10. The simulations were done at a constant ratio $h_r/T = 0.35$.

As was pointed out in¹⁰ it is of paramount importance to perform an extensive disorder average, since quantities like the susceptibility χ are non-self-averaging in this model. Therefore at least 1000 samples for each temperature and system size were used. Equilibration was checked by starting each sample with two different initial configurations, one with all spins down and the other with all spin up, and running as long as both ‘‘replica’’ yield the same values for all thermodynamic quantities

of interest. For $L = 16$ up to $2 \cdot 10^6$ Monte Carlo sweeps were necessary to fulfill this criterion.

The following quantities were calculated for each disorder realization: The average magnetization per spin $\langle M \rangle$, its square $\langle M^2 \rangle$, the average energy per spin $\langle E \rangle$ and its square $\langle E^2 \rangle$. The angular brackets, $\langle \dots \rangle$, denote a thermal average for a single random field configuration and $M = 1/N \sum_{i=1}^N S_i$, $E = H(\underline{S})/N$ and $N = L^d$. From these data we get the specific heat per spin, C , the susceptibility χ , the disconnected susceptibility, χ_{dis} , and the order parameter, m , as follows

$$[C]_{\text{av}} = N \left\{ [\langle E^2 \rangle]_{\text{av}} - [\langle E \rangle^2]_{\text{av}} \right\} / T^2, \quad (16)$$

$$[m]_{\text{av}} = [|\langle M \rangle|]_{\text{av}}, \quad (17)$$

$$[\chi]_{\text{av}} = N \left\{ [\langle M^2 \rangle]_{\text{av}} - [\langle M \rangle^2]_{\text{av}} \right\} / T, \quad (18)$$

$$[\chi_{\text{dis}}]_{\text{av}} = N [\langle M^2 \rangle]_{\text{av}}, \quad (19)$$

where $[\dots]_{\text{av}}$ denotes the average over different random field configurations. The finite size scaling function of any quantity $A(T, L)$, which behaves in the infinite system like $A_\infty \sim t^{-a}$ by approaching the critical temperature, reads

$$A(T, L) = L^{\alpha/\nu} \tilde{A}(tL^{1/\nu}). \quad (20)$$

In case of the specific heat the scaling function $\tilde{C}(x)$ has a maximum at some value $x = x^*$. For each lattice-size we estimate the temperature $T^*(L)$, where $T^2[C]_{\text{av}}$ is maximal. Since $t^*(L) L^{1/\nu} = x^*$ we obtain in this way the critical temperature T_c and the correlation length exponent ν from

$$t^*(L) \equiv T^*(L) - T_c = x^* L^{-1/\nu}. \quad (21)$$

We denote the value of $T^*(L)^2 [C]_{\text{av}}$ at this temperature $T^*(L)$ by $[C^*]_{\text{av}}$ and similarly for the other quantities in Eq. (16-19): $[\chi^*]_{\text{av}} \equiv T^*(L) [\chi(L, T^*(L))]_{\text{av}}$, $[\chi_{\text{dis}}^*]_{\text{av}} \equiv [\chi_{\text{dis}}(L, T^*(L))]_{\text{av}}$ and $[m^*]_{\text{av}} \equiv [m(L, T^*(L))]_{\text{av}}$. Then one expects the following behavior:

$$[C^*]_{\text{av}} \sim L^{\alpha/\nu} \tilde{C}(x^*), \quad (22)$$

$$[\chi^*]_{\text{av}} \sim L^{2-\eta} \tilde{\chi}(x^*), \quad (23)$$

$$[\chi_{\text{dis}}^*]_{\text{av}} \sim L^{4-\bar{\eta}} \tilde{\chi}_{\text{dis}}(x^*), \quad (24)$$

$$[m^*]_{\text{av}} \sim L^{-\beta/\nu} \tilde{m}(x^*). \quad (25)$$

Through the size dependence of $[C^*]_{\text{av}}$, $[\chi^*]_{\text{av}}$, $[\chi_{\text{dis}}^*]_{\text{av}}$ and $[m^*]_{\text{av}}$ we obtain the exponents α , η , $\bar{\eta}$ and β . In the vicinity of x^* the scaling function $\tilde{C}(x)$ can be approximated by a parabola. Therefore three temperatures near the maximum of the specific heat are enough to determine the values of $T^*(L)$ as well as $[C^*]_{\text{av}}$ etc. Let us assume that we measured $C_1 \pm \Delta_1$, $C_2 \pm \Delta_2$ and $C_3 \pm \Delta_3$ for temperatures $T_1 < T_2 < T_3$. In order to get a reliable estimate for $\bar{C}(L)$ as well as its errorbar we have to have $C_1 + \Delta_1 < C_2 - \Delta_2$ and $C_3 + \Delta_3 < C_2 - \Delta_2$, hence it is important to have very small statistical errors Δ_1 ,

Δ_2 and Δ_3 . The difference between the temperatures should be small, otherwise the second order polynomial approximation fails, but not too small, since then the above requirement for the difference between C_1 , C_2 and C_3 cannot be fulfilled. We used $T_2 - T_1 = T_3 - T_2 = 0.1$ for the small lattice sizes ($L < 10$) and 0.05 for the larger sizes. Once $T^*(L)$ is determined, the value of the quantities in (22-25) are again determined by fitting a second order polynomial. Finally, the exponents are determined via least square fits of the data obtained to the functional forms given in (22-25).

III. THE CRITICAL EXPONENTS

First we determine the temperature $T^*(L)$, where the maximum of the specific heat occurs and fit the correlation length exponent ν in such a way that the data for $T^*(L)$ lie on a straight line if plotted against $L^{-1/\nu}$. Then relation (21) is fulfilled and T_c can be read off from the intersection of this line with the y -axis. The result is depicted in figure (1), one obtains

$$\nu = 1.1 \pm 0.2 \quad \text{and} \quad T_c = 3.695 \pm 0.02. \quad (26)$$

Next we analyse the size-dependence of maximum of the specific heat. According to (22) one should be able to read off the exponent-ratio α/ν from the slope of a straight line fit in a log-log plot of $[C^*]_{\text{av}}$ versus L . The first observation is that this procedure does not work since the data points show a significant negative curvature in a log-log plot, indicating a much weaker dependency than algebraic. In reminiscence of the experimental finding of a *logarithmic* divergence of the specific heat (i.e. $\alpha = 0$) we plotted $[C^*]_{\text{av}}$ versus $\log(L)$, and still found a (now less pronounced) negative curvature in the data points, indicating a still weaker or even no divergence. Finally we hypothesized a cusp-like singularity, i.e.

$$c_\infty - [C^*]_{\text{av}} \sim L^{\alpha/\nu} \quad (27)$$

with $\alpha < 0$. The result of the corresponding fitting procedure is shown in figure 2. As one can see the data are fully consistent with this type of dependency and we get

$$\alpha/\nu = -0.45 \pm 0.05 \quad \text{and} \quad c_\infty = 30.4 \pm 0.1. \quad (28)$$

With the estimate for ν from (26) it is $\alpha = -0.5 \pm 0.2$. Although the ratio α/ν can be determined quite accurately, the value for α alone depends on ν which has a much larger large error bar.

According to (23) the susceptibility at the temperature $T^*(L)$ should diverge algebraically, and the exponent η is obtained by a least square straight line fit of $[\chi^*]_{\text{av}}$ versus L in a log-log plot, which is depicted in figure 3. The result is

$$\eta = 0.50 \pm 0.05, \quad (29)$$

from which one obtains via (10) $\gamma = 1.7 \pm 0.2$.

The finite size scaling behavior of χ near the critical temperature is expected to be

$$[\chi]_{\text{av}}(T, L) \approx L^{2-\eta} \tilde{\chi}(L^{1/\nu}(T - T_c)) . \quad (30)$$

In figure 4 the corresponding finite size scaling plot using the values for T_c , ν and η from (26) and (29) is shown.

The disconnected susceptibility at $T^*(L)$ is depicted in figure 5, which should diverge according to (24) with system size. Via a least square fit of the data to a straight line in the log-log plot one obtains the estimate

$$\bar{\eta} = 1.03 \pm 0.05 . \quad (31)$$

With the scaling relation (7) one can estimate θ to be

$$\theta = 1.5 \pm 0.1 , \quad (32)$$

which is in good agreement with the value $\theta = d/2$ mentioned in the last section.

Comparing our values for η (29) and $\bar{\eta}$ (31) one notes that the relation (14) might be fulfilled, which would support the two-exponent scaling scenario mentioned in the last section. In order to check this we calculated the amplitude ratio

$$\mathbf{A} = \lim_{T \rightarrow T_c} \frac{[\chi_{\text{dis}}]_{\text{av}}}{[\chi]_{\text{av}}^2 (h_r/T)^2} . \quad (33)$$

as suggested in²³, where in an extensive high-temperature analysis it was found that $A = 1$, implying strong evidence for two-exponent scaling. The finite size scaling form of (33) is $\mathbf{A}(L, T) = \tilde{\mathbf{A}}(L^{1/\nu}(T - T_c))$ and therefore we expect

$$\mathbf{A}^*(L) \equiv \mathbf{A}(L, T^*(L)) = 1 \quad (34)$$

independent of system size. The result that we obtain from our MC-data is table 1:

L	A^*	ΔA^*
4	1.19	0.22
6	1.14	0.23
8	1.10	0.33
10	1.12	0.29
12	1.00	0.26
16	0.80	0.27

TABLE I: The amplitude ratio $A^*(L) = A(L, T^*(L))$ and its estimated error for different system sizes.

As one can see A^* is close to one, which supports the equality (14). Because of the large errorbars the slight decrease in the estimate of A^* with increasing system size seems not to be significant.

From equation (31) one concludes that the disconnected susceptibility diverges roughly with the volume of the system, since from (11) one obtains $\bar{\eta}/\nu = 4 - \bar{\eta} \approx 3 = d$. If one looks at equation (19), where χ_{dis} is defined,

this implies that $[\langle M^2 \rangle]_{\text{av}} = \chi_{\text{dis}}/L^d$ is then independent of system size at the critical temperature. Since the magnetization is defined in a similar manner (17), namely the square replaced by the modulus, it does not come as a surprise that one observes that also the magnetization is also independent of system size at the critical point. This connection manifests itself in the relation (12), which predicts $\beta \approx 0$ if $\bar{\eta} \approx 1$. By looking at $[m^*]_{\text{av}}$ as a function of L we cannot detect any significant variation with system size. As an even stronger evidence we show in figure 6 a finite size scaling plot of the magnetization according to

$$[m]_{\text{av}}(T, L) \approx \tilde{m}(L^{1/\nu}(T - T_c)) \quad \text{if } \beta = 0 , \quad (35)$$

using the values for T_c and ν estimated above. Also by studying the probability distribution of the magnetization in the next section, we see that that the system in the thermodynamic limit is already ordered at T_c . Finally, if the transition is first order, one expects $\eta = 1/2^{25}$, which is in agreement with our estimate (29).

Finally we study the dimensionless coupling constant or Binder cumulant

$$g(T, L) = 0.5 \left\{ 3 - \frac{[\langle M^4 \rangle]_{\text{av}}}{[\langle M^2 \rangle]_{\text{av}}^2} \right\} , \quad (36)$$

which is expected to be independent of size at T_c . In figure 7 we show the result for three different system sizes as a function of temperature. The intersection of the curves of the two largest system sizes lie very close to the estimated value of $T_c = 3.695$.

One observes that close to the critical temperature the value of the cumulant g lies already very close to 1. This means that the probability distribution for the order parameter is centered around a non-vanishing value for the magnetization, implying a large degree of magnetic order already at T_c . This is fully compatible with $\beta = 0$ and a discontinuous jump in the expectation value for the disorder-averaged magnetization at the critical temperature

IV. PROBABILITY DISTRIBUTIONS

As mentioned above the susceptibility is a highly non-selfaveraging quantity, which can be demonstrated by looking at the distribution $P(\chi)$ for the probability to find a value χ for the susceptibility of one sample (i.e. realization of the disorder). $P(\chi)$ is far from being a Gaussian distribution and it possesses pronounced long tails as shown in figure 8 (see also²⁵).

This is one of the predictions of the droplet theory^{4,5}: With a probability proportional to $L^{-\theta}$ a sample has a vanishing thermodynamic expectation value for the magnetization leading to a strongly enhanced susceptibility that is in this case equal to the disconnected susceptibility, as can be seen from its definition (18,19). This argument leads to the equation (7). Moreover it says that the

second moment $[\chi^2]_{\text{av}}$ of the distribution $P(\chi)$ is dominated by these rare events occurring with probability $L^{-\theta}$ and giving a contribution proportional to the square of the disconnected susceptibility, i.e. $(L^{4-\bar{\eta}})^2$. This gives

$$[\chi^2]_{\text{av}}(L, T^*(L)) \sim L^\zeta, \quad (37)$$

with $\zeta = -\theta + 2(4 - \bar{\eta}) \approx 4.5$ via (32) and (31). This gives a much larger contribution than the square of the mean value $[\chi]_{\text{av}}^2 \sim L^{2(2-\eta)} \approx L^{3.0}$. By explicitly calculating $[\chi^2]_{\text{av}}(T^*L, L)$ with our MC-data we get an estimate of $\zeta = 4.0 \pm 0.2$, which is indeed closer to the above droplet prediction of 4.5.

The scaling hypothesis concerning the probability distribution of the magnetization can be checked by inspecting the latter directly. In figure 9 we show the probability distribution of the magnetization for different system sizes at a temperatures close to $T^*(L)$. Let us focus at the moment on the behavior of $P_L(m)$ at zero magnetization. Note that m is defined as the modulus of the thermodynamic expectation value of the fluctuating quantity M and can thus take on only positive values.

At a usual second order phase transition $P_L(m, T^*(L))$ would have a peak at $m = 0$ with a width that is proportional $\chi^*(L)/L^d \sim L^{2-\eta-d}$. Thus this peak narrows and gains more weight with increasing system size. Here it is quite contrary, the peak develops at a nonzero value m_∞ for the magnetization. If it would be a conventional Gaussian distribution centered around this nonvanishing most probable value for the magnetization, its value at $m = 0$ would decrease exponentially with system size: $P_0^*(L) \equiv P_L(m = 0, T^*(L)) \propto \exp(-m_\infty^2 L^{d-2+\eta})$. However, according to the above mentioned scaling theory, one expects

$$P_0^*(L) \sim L^{-\theta}, \quad (38)$$

which is a much slower decay. In order to improve the statistics we estimated $P_0^*(L)$ via $P(m = 0) \approx \Delta m^{-1} \int_0^{\Delta m} dm P(m)$ with $\Delta m = 0.2 - 0.3$. In figure 10 we depict the result from which we conclude that (38) obeyed and we estimate $\theta = 1.0 \pm 0.1$, which is smaller than the value (32) obtained by the relation (7). It is clear that a nonvanishing Δm overestimates $P_0^*(L)$ more for larger system sizes, which might explain this discrepancy.

Finally we turn our attention to the variation of $P(m)$ with temperature. According to ref.^{26,27} the probability distribution of the order parameter provides a mean to discriminate between a first and a second order phase transition. At a usual first order transition one expects a phase-coexistence at the critical point, which means that $P(m)$ has two significant peaks, one at zero (representing the high temperature phase) and one at a positive value $m_\infty > 0$ (representing the low temperature phase). In this case the effective transition temperature $T_c(L)$ of the finite system can be identified by the temperature, where both peaks have equal weight²⁷.

If we look at figure 11, where $P_{L=16}(m)$ is shown for various temperature values, we detect no sign of a characteristic double-peak structure mentioned above. On the contrary, there is only a single peak moving continuously to the right with decreasing temperature. Thus we conclude that phase-coexistence at T_c can be excluded in the RFIM, although the magnetization jumps discontinuously there. Hence there is a discontinuity in one of the derivatives of the free energy (namely with respect to a homogeneous external magnetic field), which means that the transition is first order in a strict sense. Nevertheless it is a quite unusual first order phase transition: neither a latent heat nor a phase-coexistence at T_c could be detected in our simulations.

We would like to remark that our findings for the probability distribution $P_L(m, T)$ are fully compatible with the scenario, which is suggested by the droplet theory^{4,5} — in particular the systematic decrease of the probability for samples with zero magnetization (38). Once we accept that $P_L(m = 0)$ shrinks to zero at T_c in the limit $L \rightarrow \infty$ the weight of the distribution has to cumulated at a nonzero most probable value for m . As we have discussed this implies a discontinuous jump of the average magnetization at T_c . Thus one might speculate that our finding $\beta = 0$ is an intrinsic feature of the droplet theory, although such a possibility has not been discussed yet to our knowledge.

Another paradigm of usual first order phase transitions is that the correlation length stays finite at T_c , although it might become very large (for a counter-example see²⁸). In this case the scaling analysis performed in the last section is unjustified, since it relies on a second order phase transition scenario with a diverging correlation length. However, since neither the specific heat nor the order parameter probability distribution behaves as usual at a first order transition there seems also to be no reason us for to expect a finite correlation length at T_c . Finally let us mention that we also looked at the probability distribution of the internal energy. Here no remarkable behavior could be observed.

V. DISCUSSION

To summarize we list the values for the critical exponents that we have calculated in table II together with those for the binary distribution obtained in¹⁰. Let us compare these numbers with other known values from the literature: $\eta = 0.25 \pm 0.03$, $\bar{\eta} \sim 0.8$, $\gamma = 1.7 \pm 0.2$ and indications of a first order transition from MC-simulations of the RFIM⁹; $\eta = 0.5 \pm 0.1$ and $\bar{\eta} = 1.0 \pm 0.3$ from MC-simulations of the DAFF⁷; $\bar{\eta} = 1.1 \pm 0.1$ and $\nu = 1.0 \pm 0.1$ from a ground-state investigation via combinatorial optimization⁸; $\gamma = 1.9 - 2.2$ from real space renormalization group calculations²⁵; $\gamma = 2.1 \pm 0.2$, $\bar{\gamma} = 4.2 \pm 0.4$ from high temperature series expansion²³; $\nu = 1.25 \pm 0.11$, $\bar{\eta} = 0.89 \pm 0.10$ and $\eta = 0.4 \pm 0.8$ from

a weighted mean field theory³⁰. Our estimates are well compatible with all of these results.

	Gaussian		Binary	
η	0.50	± 0.05	0.56	± 0.03
$\bar{\eta}$	1.03	± 0.05	1.00	± 0.06
θ	1.53	± 0.1	1.56	± 0.1
ν	1.1	± 0.2	1.6	± 0.3
γ	1.7	± 0.2	2.3	± 0.3
$\bar{\gamma}$	3.3	± 0.6	4.8	± 0.9
β	0.00	± 0.05	0.00	± 0.05
α	-0.5	± 0.2	-1.0	± 0.3

TABLE II: The critical exponents for the Gaussian distribution considered in this paper and for the binary distribution investigated in ref.¹⁰, both for the constant field-strength/temperature ratio $h_r/T = 0.35$

The first important observation is that the results obtained for a Gaussian and a binary distribution do not differ significantly. In particular the indications for a discontinuity in the magnetization $\beta = 0$ detected for the binary distribution in ref.¹⁰ are also present for the Gaussian distribution investigated in this paper. This is a crucial point with regards to mean-field theory¹⁹, where an essential difference between the two kinds of distributions is predicted: In contrast to the continuous case with nonvanishing weight at zero field strength the binary distribution is expected to have a tricritical point, where the transition changes from second to first order. Our conclusion in this paper is that in three dimensions both distributions lead to identical results for the investigated field strength.

Our estimate for the correlation length exponent ν has a rather large errorbar, which is also the main source for the error in the values for γ , $\bar{\gamma}$ and α . One notes also a discrepancy between the values of ν for the Gaussian and for the binary distribution, but they remain compatible within the errorbars. The Schwartz-Soffer inequality $\bar{\gamma} \leq 2\eta$ seems to be fulfilled as an equality, which supports the two-exponent scaling scenario, as also found in²³. An explicit calculation of the amplitude ration in section III gives further evidence in this respect.

The analysis of the probability distribution of the susceptibility showed pronounced long tails as predicted by the scaling theories^{4,5}. The source for these long tails are rare samples possessing a vanishing net-field and thus having a vanishing expectation value for the magnetization. In fact these rare samples provide the dominant contribution to the higher moments of the distribution, which we checked explicitly. The analysis of the probability distribution of the magnetization supports this picture and shows that the probability of these rare samples indeed decays like $L^{-\theta}$ with system size, where θ is an exponent whose value turns out to be compatible with other predictions of the scaling theory.

It turns out that the magnetization exponent β is zero, which means that the magnetization jumps dis-

continuously from zero to a finite value at the critical temperature. Although this might be called a first order phase transition a closer inspection of the probability distribution of the magnetization revealed the absence of a double-peak structure characterizing the phase-coexistence usually present at a first order phase transition.

Furthermore, at a first order phase transition the specific heat usually diverges with the volume of the system¹¹, but the exponent α is negative, which means that the specific heat does not diverge at T_c . By means of birefringence techniques Belanger et al.¹⁴ concluded from their experiments on $\text{Fe}_{0.47}\text{Zn}_{0.53}\text{F}_2$ that $\alpha = 0$ (i.e. a logarithmic divergence of the specific heat). Only recently it was shown¹⁵ that the same kind of experiments on $\text{Fe}_{0.85}\text{Mg}_{0.15}\text{Br}_2$ are better compatible with a cusp like singularity of the specific heat and $\alpha = -1$, concurring with the value reported in table II. However, this value for α together with the other estimates in table II would violate the modified hyper-scaling relation (4). Moreover, Schwartz²² derived an exact inequality $2 - \alpha \leq \nu(d - 2 + \eta)$ and accepting $\eta \approx 0.5$ (since this result has a much smaller errorbar than ν) it would imply $\nu \geq 2$, which is a rather large value. Indeed in a recent Migdal-Kadanoff²⁹ such a large exponent was found: $\nu = 2.25$, and also report $\alpha = -1.37$ and $\beta = 0.02$, consistent with table II. However, a value for α that is negative and large in modulus causes serious difficulties with respect to the Rushbrooke relation (13) and the more rigorous Rushbrooke inequality $\alpha + 2\beta + \gamma \geq 2$ ³¹.

Let us conclude with the remark that this investigation on one hand confirms the picture of the phase transition scenario found in ref.¹⁰. On the other hand it poses some serious puzzles concerning various scaling relations for the exponents that still remain to be solved in the future. In addition quite recently the possibility of an intermediate spin glass phase, located between the paramagnetic and the ferromagnetic phase has been discussed^{32,33}. It seems to us to be quite important to clarify the consequences of the existence such a phase, which is supposed to possess a *finite* correlation length, for the nature of the transition considered here.

ACKNOWLEDGEMENT

I would like to thank A. P. Young for his encouragement and many extremely helpful discussions. The computations were done on the Intel Paragon System from the Supercomputer center (HLRZ) at the Forschungszentrum Jülich. This work was performed within the SFB 341 Köln-Aachen-Jülich, supported by the DFG.

-
- ¹ D. P. Belanger and A. P. Young, *J. Magn. Magn. Mat.* **100**, 272 (1991), H. Rieger, *Monte Carlo Studies of Spin Glasses and Random Field Systems* in: *Ann. Rev. Comp. Phys.* II, World Scientific, Singapore (1995).
- ² J. Bricmont and A. Kupiainen, *Phys. Rev. Lett.* **59** 1829 (1987).
- ³ A. Aharony, Y. Imry and S. K. Ma, *Phys. Rev. Lett.* **37**, 1364 (1976); A. P. Young, *J. Phys. C* **10**, L257 (1977); G. Parisi and N. Surlas, *Phys. Rev. Lett.* **43**, 744 (1979).
- ⁴ J. Villain, *J. Physique* **46**, 1843 (1985).
- ⁵ D. S. Fisher, *Phys. Rev. Lett.* **56**, 416 (1986).
- ⁶ A. J. Bray and M. A. Moore, *J. Phys. C* **18**, L927 (1985).
- ⁷ A. T. Ogielski and D. A. Huse, *Phys. Rev. Lett.* **56**, 1298 (1986).
- ⁸ A. T. Ogielski, *Phys. Rev. Lett.* **57**, 1251 (1986).
- ⁹ A. P. Young and M. Nauenberg, *Phys. Rev. Lett.* **54**, 2429 (1985).
- ¹⁰ H. Rieger and A. P. Young, *J. Phys. A* **26**, 5279 (1993).
- ¹¹ M. Nauenberg and B. Nienhuis, *Phys. Rev. Lett.* **33**, 944 (1974).
- ¹² S. Fishman and A. Aharony, *J. Phys. C* **12**, L729 (1979).
- ¹³ J. Cardy, *Phys. Rev. B* **29**, 505 (1985).
- ¹⁴ D. P. Belanger, A. R. King and V. Jaccarino, *Phys. Rev. B* **31**, 4538 (1985). P. Pollack, W. Kleemann and D. P. Belanger, *Phys. Rev. B* **38**, 4773 (1988).
- ¹⁵ M. Karszewski, J. Kushauer, Ch. Binek, W. Kleemann and D. Bertrand, *J. Phys. C* **6**, L75 (1994).
- ¹⁶ R. J. Birgeneau, R. A. Cowley, G. Shirane and H. Yoshizawa, *Phys. Rev. Lett.* **54**, 2174 (1985).
- ¹⁷ J. P. Hill, Q. Feng, R. J. Birgeneau and T. R. Thurston, *Phys. Rev. Lett.* **70**, 3655 (1993); *Z. Phys. B* **92**, 285 (1993).
- ¹⁸ W. Kleemann, *Int. J. Mod. Phys. B* **7**, 2469 (1993).
- ¹⁹ A. Aharony, *Phys. Rev. B* **18**, 3318 (1978).
- ²⁰ Y. Imry and S. K. Ma, *Phys. Rev. Lett.* **35**, 1399 (1975).
- ²¹ M. Schwartz and A. Soffer, *Phys. Rev. Lett.* **55**, 2499 (1985).
- ²² M. Schwartz, *J. Phys. C* **18**, 135 (1985); M. Schwartz and A. Soffer, *Phys. Rev. B* **33**, 2059 (1986); M. Schwartz, M. Gofman and T. Nattermann, *Physica A* **178**, 6 (1991). M. Schwartz, *Europhys. Lett.* **15**, 777 (1994).
- ²³ M. Gofman, J. Adler, A. Aharony, A. B. Harris et al., *Phys. Rev. Lett.* **71**, 1569 (1993).
- ²⁴ H. Rieger, *J. Stat. Phys.* **70**, 1063 (1993).
- ²⁵ I. Dayan, M. Schwartz and A. P. Young, *J. Phys. A* **26**, 3093 (1993).
- ²⁶ K. Binder and D. P. Landau, *Phys. Rev. B* **30**, 1477 (1984).
- ²⁷ M. S. S. Challa, D. P. Landau and K. Binder, *Phys. Rev. B* **34**, 1841 (1986).
- ²⁸ P. W. Anderson and G. Yuval, *J. Phys. C* **4**, 607 (1971).
- ²⁹ M. S. Cao and J. Machta, *Phys. Rev. B* **48**, 3177 (1993).
- ³⁰ D. Lancaster, E. Marinari and G. Parisi, *Weighted Mean Field Theory for the RFIM*, cond-mat/9412069.
- ³¹ G. S. Rushbrooke, *J. Chem. Phys.* **39**, 842 (1963).
- ³² M. Mézard and A. P. Young, *Europhys. Lett.* **18**, 653 (1992).
- ³³ M. Mézard and R. Monasson, *Phys. Rev. B* **50**, 7199 (1994).

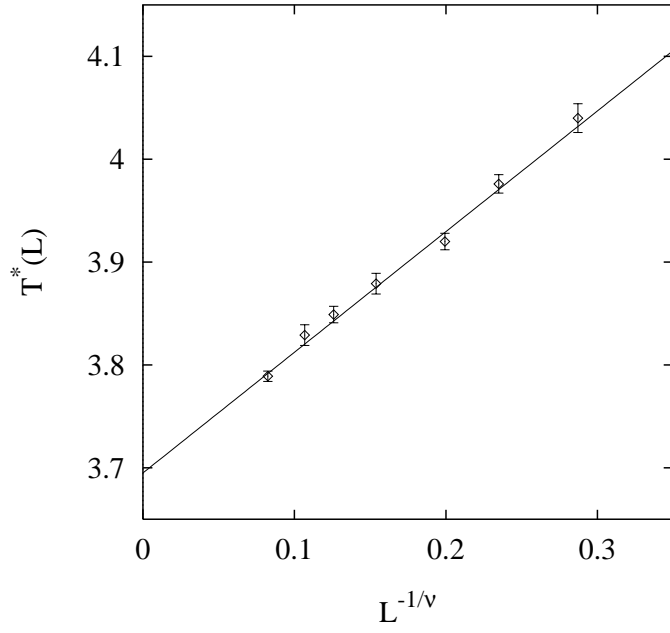


FIG. 1. The temperature $T^*(L)$, where the specific heat attains its maximum, versus $L^{1/\nu}$, with ν as in (26). From right to left one has $L = 4, 5, 6, 8, 10, 12$ and 16 . The full line is a least square straight line fit.

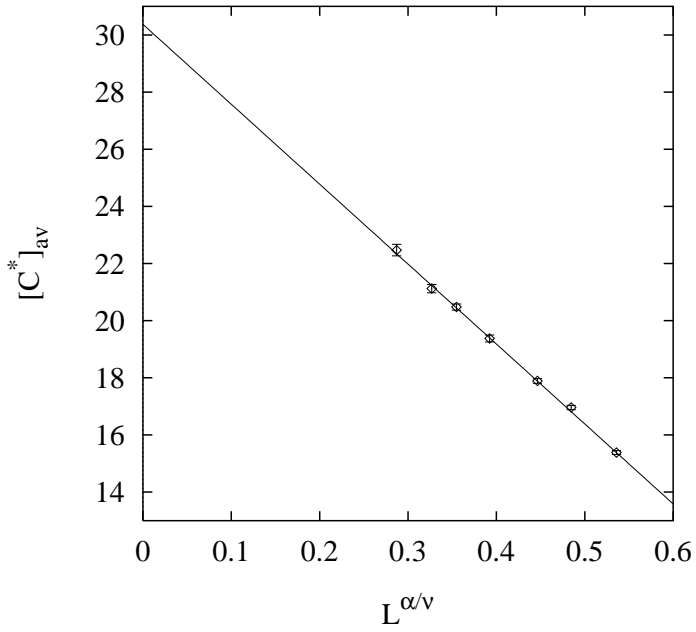


FIG. 2. The maximum of the specific heat $[C^*]_{av}$ versus $L^{\alpha/\nu}$ with α/ν as in (26). From right to left one has $L = 4, 5, 6, 8, 10, 12$ and 16 . The full line is a least square straight line fit.

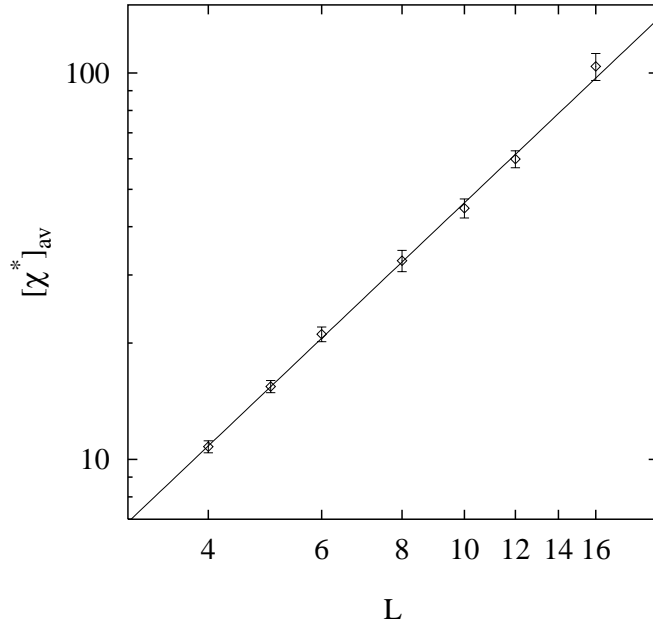


FIG. 3. The value of the susceptibility $[\chi]_{\text{av}}$ at the temperature $T^*(L)$ versus system size L in a log-log plot. The full line is a least square straight line fit, which gives a slope of 1.55 ± 0.05 that is an estimate for $2 - \eta$ according to (23).

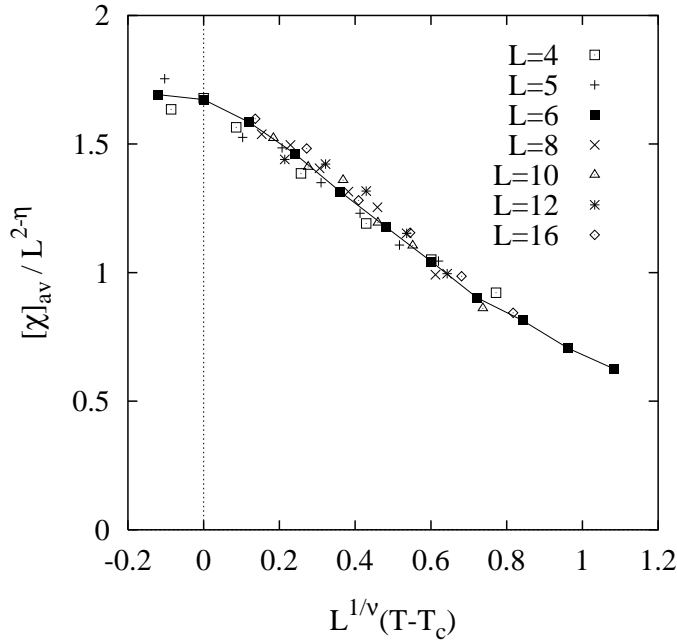


FIG. 4. A scaling plot of the susceptibility $[\chi]_{\text{av}}$ with the parameters for T_c , ν and η given in (21) and (23). The full line connects only the points for $L = 6$ as a guide for the eyes.

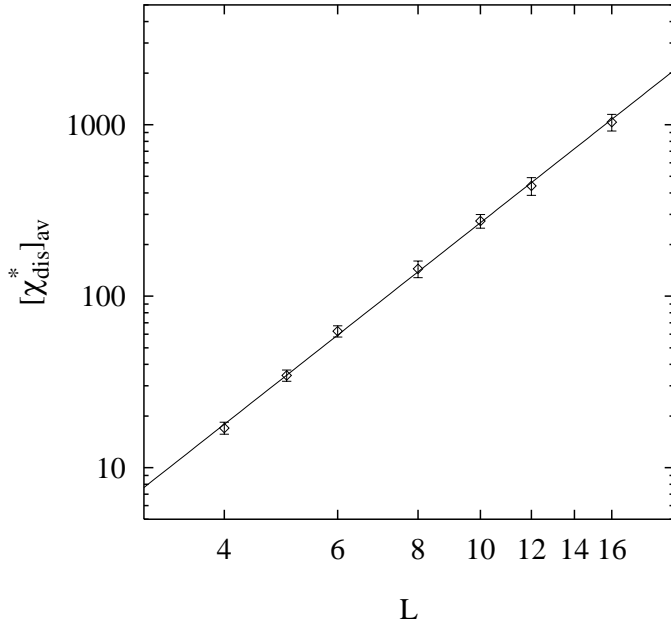


FIG. 5. The disconnected susceptibility $[\chi_{\text{dis}}^*]_{\text{av}}$ at the temperature $T^*(L)$ versus L in a log-log plot. The full line is a least square straight line fit, which gives a slope of 2.97 ± 0.08 that is an estimate for $4 - \bar{\eta}$ according to (24).

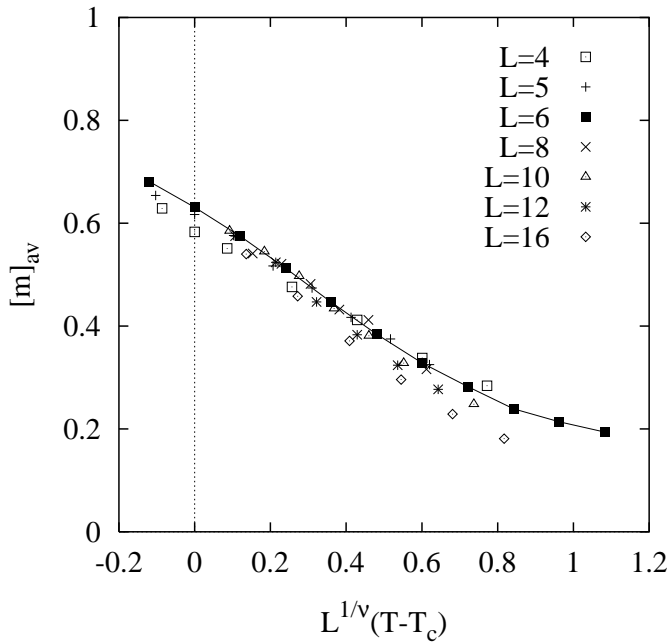


FIG. 6. A scaling plot of the magnetization $[M]_{\text{av}}$ with the parameters for T_c and ν given in (21). The full line connects only the points for $L = 6$ as a guide for the eyes. Note that the data for $[M]_{\text{av}}$ are *not* rescaled by a factor $L^{-\beta/\nu}$, implying that indeed $\beta = 0$.

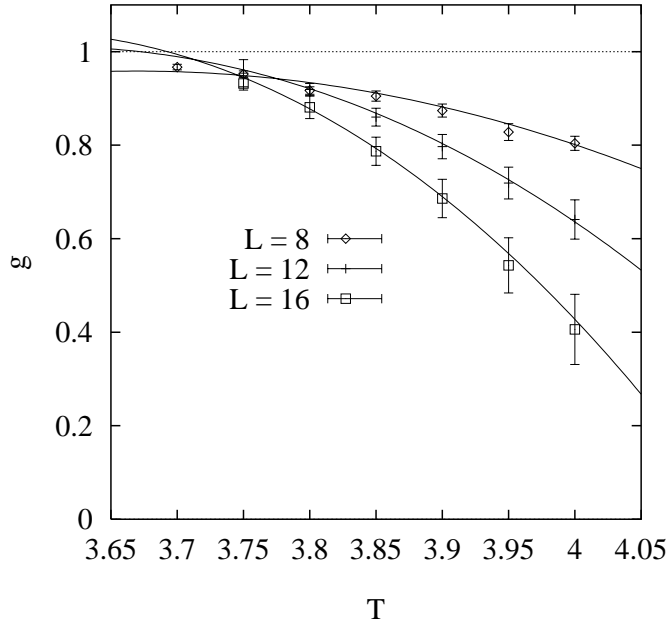


FIG. 7. The cumulant g as defined in (36) versus temperature for three different system sizes. The full curves are least square fits of third order polynomials to the data points. The intersection of the $L = 16$ and $L = 12$ curves lies already close to the estimated critical temperature $T_c = 3.695$ (21).

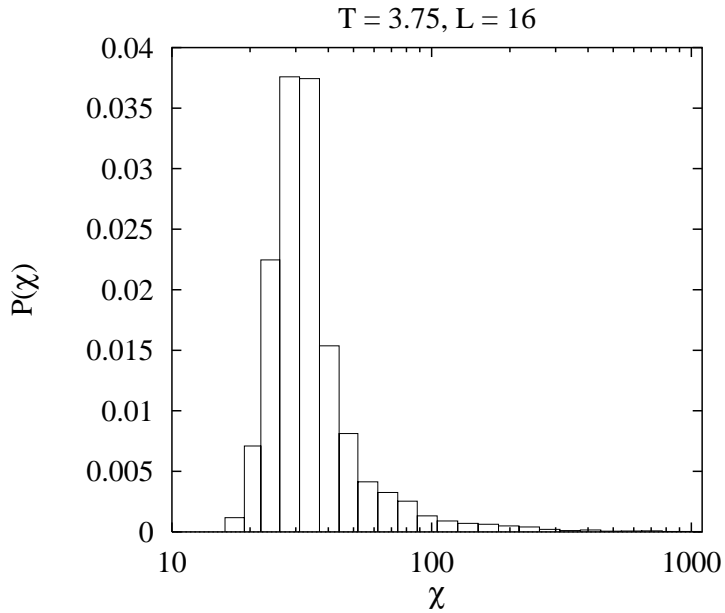


FIG. 8. The probability distribution $P(\chi)$ for $L = 16$ at the temperature $T = 3.75 \approx T^*(L = 16)$. Note the logarithmic scale of the abscissa.

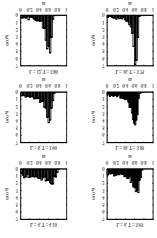


FIG. 9. The probability distribution $P_L(m)$ for increasing system sizes close to the temperature $T^*(L)$. The tendency towards a dominant peak at nonvanishing magnetization for increasing system size is obvious.

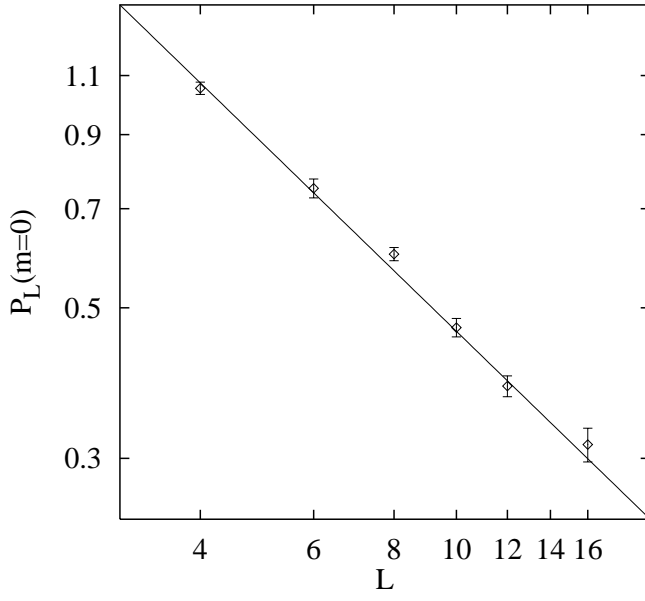


FIG. 10. The probability $P_L(m = 0, T = T^*(L))$ versus system size L in a log-log plot. The full curve is a least square straight line fit with slope $\theta = -1.0 \pm 0.1$.

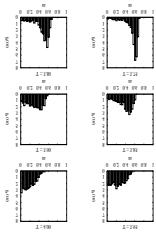


FIG. 11. The probability distribution $P(m)$ for $L = 16$ at different temperatures. Note that $T = 3.80$ is slightly above $T^*(L = 16)$ and $T = 3.75$ is slightly below it, but still above the estimated value for $T_c = 3.695$.